Electronic Supplementary Material (ESI) for Physical Chemistry Chemical Physics.

Supporting information for publication

1. The morphology and crystallinity of ZnO and Cu_2O film

The XRD data of the ZnO inverse opal (IO) structures with the ZnO planar film were reported bellow. Similar crystal structure (i.e. P63mc space group with hexagonal crystal structure) is observed between ZnO IO and ZnO planar film. The X-ray diffraction intensity for planar ZnO was lower due to thinner film as compared to ZnO IO. The XRD spectra of Cu_2O film shows high crystallinity of Cu_2O film deposited by electrodeposition method.

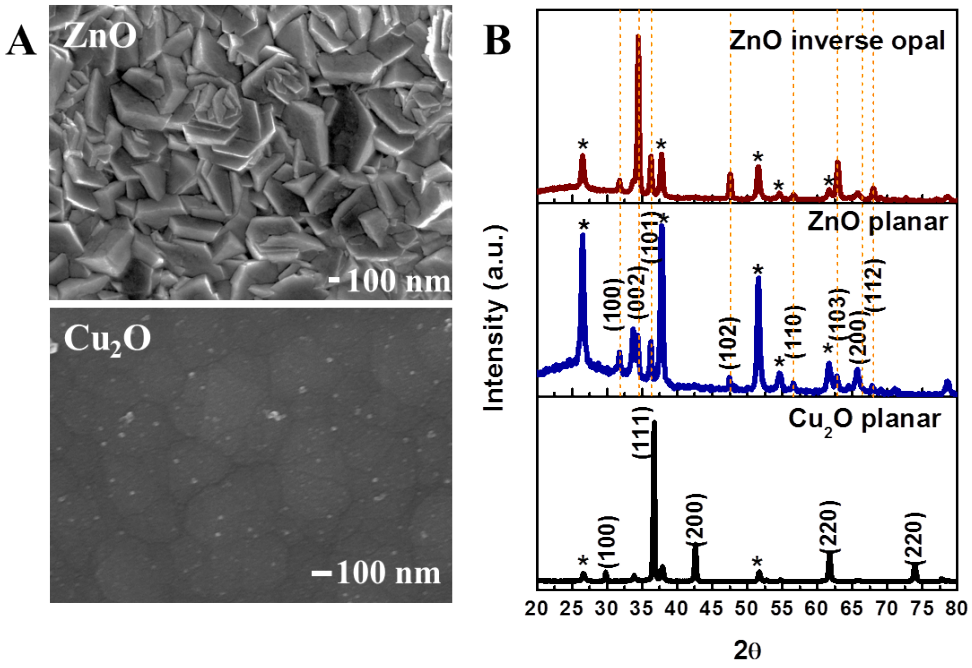

Figure S1. The morphology of planar ZnO and Cu_2O film (A) together with the XRD spectra (B) of planar ZnO, inverse opal ZnO and Cu_2O film. The * indicates the contribution of X-ray spectra from the substrate (FTO).

2. Study on the depletion width of the ZnO/Cu_2O solar cell

Capacitance versus voltage measurement was done on the deposited ZnO and Cu_2O film on FTO substrate inside polycarbonate solvent. Mott-Schottky analysis was constructed to probe the carrier density of both ZnO and Cu_2O prepared by electrochemical deposition. For the analysis, $\varepsilon_{ZnO} = 3.8$ and $\varepsilon_{Cu_2O} = 7.11$ was adopted [1,2]. A positive slope that indicated the n-type nature of ZnO with a carrier concentration of 8.5 x 10^{19} cm^{-3} was measured with a flat band potential at -0.61 V (vs Ag/AgCl). Carrier concentration (N_A) of 2.6 x 10^{18} cm^{-3} with a negative slope that

indicate the p-type semiconductor was observed for Cu_2O film. The flat band potential of Cu_2O film was measured at 0.38 V (vs Ag/AgCl). Assuming majority of the depletion width is located in Cu_2O film, the depletion width in the ZnO/Cu_2O interface was estimated according to following equation:

$$V_{bi}(p) = \frac{q\, N_A\, x_p^2}{2\, \varepsilon_{Cu_2O}}$$

Where N_D, N_A, ε_{ZnO}, and ε_{Cu_2O} are donor and acceptor concentration and absolute permittivities of ZnO and Cu_2O respectively. Assuming built in bias of about 0.4 to 0.7 V, the calculated depletion thickness is about 11 to 17 nm. This value was relatively small than the predicted depletion width value from Musselman group (10^{13} - 10^{14} cm^{-3}) [3]. The differences might come from the quality of the Cu_2O film prepared in which higher carrier concentration was observed in the current study. The modulation of Cu_2O carrier concentration with respect to the deposition parameters has been reported previously [4].

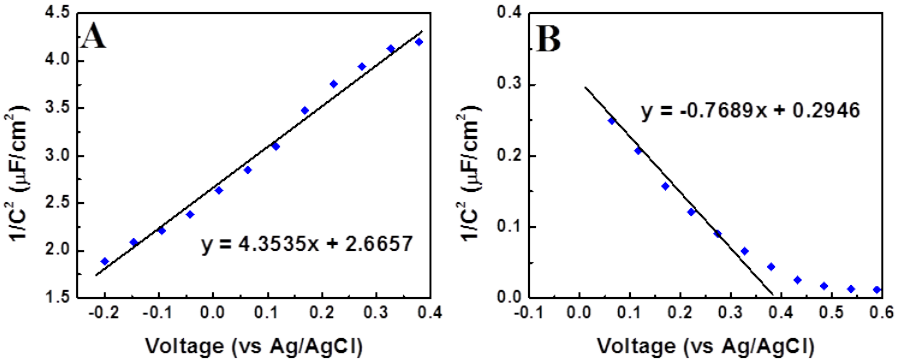

Figure S2. The Mott-Schottky plots for ZnO (A) and Cu_2O (B).

3. Investigation on the band energy alignment for ZnO/Cu_2O solar cell

The Fermi energy (E_F) level of both ZnO (4.29 eV) and Cu_2O (5.28 eV) was estimated from the flat band potential obtained from the Mott-Schottky analysis. The offset between the E_F level and the conduction band (E_{CB}) or valence band (E_{VB}) could be estimated according to equation below [5]:

$$E_F - E_{VB} = \frac{k.T}{e}.ln\frac{N_V}{N_A} \quad or \quad E_{CB} - E_F = \frac{k.T}{e}.ln\frac{N_C}{N_D}$$

where k, T, N_V, and N_C are Boltzmann constant, temperature, the effective density states at the top of the valence band, and the effective density states at the bottom of the conduction band respectively. The N_V and N_C could be calculated from equation below [5]:

$$N_V = 2\left(\frac{2.\Pi.m^*.k.T}{h^2}\right)^{3/2} \quad or \quad N_C = 2\left(\frac{2.\Pi.m^*.k.T}{h^2}\right)^{3/2}$$

where m* and h are the effective hole or electron mass and Planck constant respectively. The effective hole mass of 0.66 m_o and effective electron mass of 0.27 m_o are used for calculating the N_V of Cu_2O and N_C of ZnO respectively [6,7]. The bandgaps obtained from the Tauc plots (the $(\alpha.h.v)^2$ versus (h.v) curve) were used to calculate the E_{CB} of Cu_2O and E_{VB} or ZnO. The FTO and Au Fermi energy level (4.4eV and 5.3 eV respectively) are adopted from previous report [8,9]. The band positions of FTO/ZnO/Cu_2O/Au are represented in Figure S3.

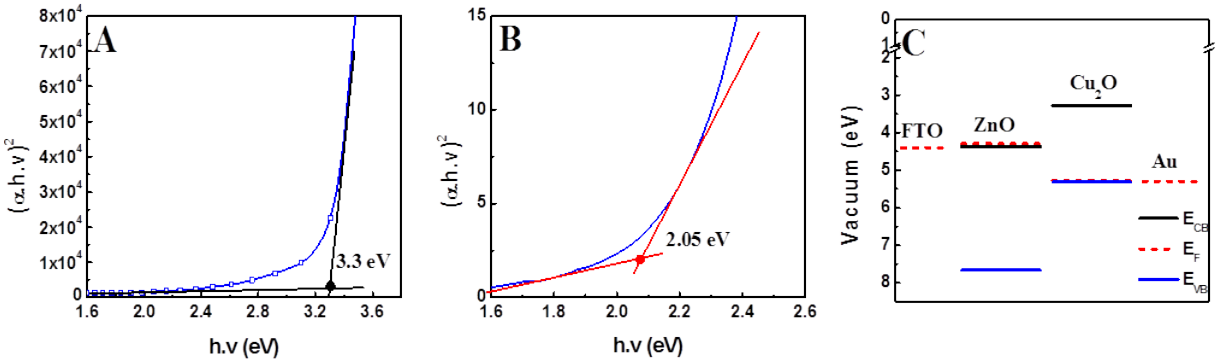

Figure S3. The Tauc plots for ZnO (A) and Cu_2O (B) obtained from UV-Vis spectroscopy measurement and the energy band alignment of FTO/ZnO/Cu_2OAu (C).

4. Impact of Cu_2O overlayer on the inverse opal devices.

To eliminate the effect of Cu_2O overlayer, 300IO3 and 300IO5 devices with similar Cu_2O overlayer (~ 800 nm) was fabricated and called 300IO3-R and 300IO5-R respectively. The results indicated similar trends with 300IO3 and 300IO5 observed. This highlighted that the Cu_2O overlayer does not play a major roles on the J_{sc} and EQE of devices with thickness ≥ 3 layers of inverse opal film as most of the light absorption occurs at the first 3 inverse opal layers.

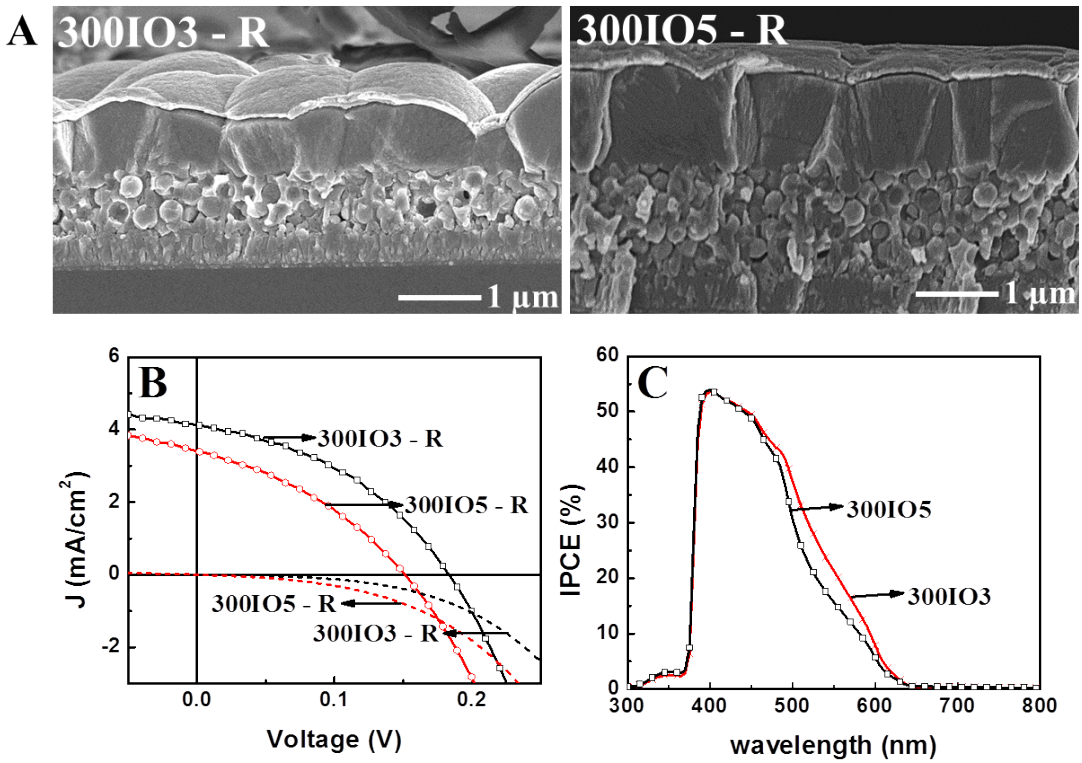

	PCE (%)	J_{sc} (mA/cm^2)	Integrated J_{sc} (mA/cm^2)	V_{oc} (V)	FF
300IO 3 - R	0.3	4.13	4.19	0.18	0.40
300IO 5 - R	0.18	3.39	3.7	0.15	0.35

Figure S4. The cross section images (A), the J-V characteristic (B), and IPCE (C) of 300IO3-R and 300IO5-R devices with similar Cu_2O overlayer.

5. The FDTD analysis of calculated absorption enhancement factor with varied IO pore diameter for 3 IO layers and 5 IO layers.

From the FDTD analysis, similar trend was observed (i.e. composite opal with diameter > 200 nm helps to magnify photon absorption near the interface) for both simulation with 3 and 5 IO layers. This confirms that majority of Cu_2O absorption occurred in the first 3 layers

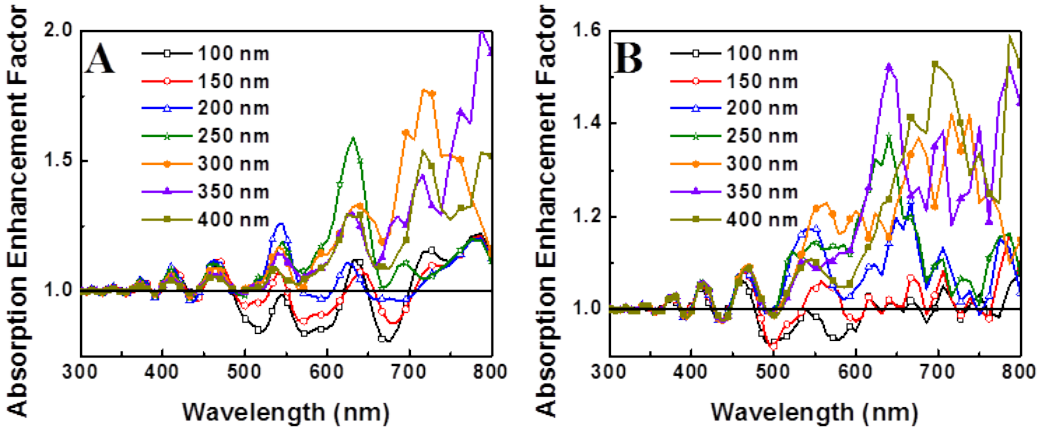

Figure S5. The calculated absorption enhancement factor for 5 IO layers (A) and 3 IO layers (B) with different IO pore diameter.

References:

(1) O'Keeffe, M. *J. Chem. Phys.* **1963**, *39*, 1789.

(2) Noh, H.; Scharrer, M.; Anderson, M.; Chang, R.; Cao, H. *Phys. Rev. B* **2008**, *77*, 1–9.

(3) Musselman, K. P.; Marin, A.; Schmidt-Mende, L.; MacManus-Driscoll, J. L. *Adv. Funct. Mater.* **2012**, *22*, 2202–2208.

(4) Jiang, T.; Xie, T.; Chen, L.; Fu, Z.; Wang, D. *Nanoscale* **2013**, *5*, 2938.

(5) Abou-ras, D.; Kirchartz, T.; Rau, U. *Advanced Characterization Techniques for thin film solar cells*; Abou-ras, D.; Kirchartz, T.; Rau, U., Eds.; Wiley-VCH Verlag GmbH & Co. KGaA: Weinheim, Germany, 2011.

(6) Hodby, J. W.; Jenkins, T. E.; Schwab, C.; Tamura, H.; Trivich, D. *J. Phys. C Solid State Phys.* **1976**, *9*, 1429.

(7) Hutson, A. R. *Phys. Rev.* **1957**, *108*, 222.

(8) Sachtler, W. M. H.; Dorgelo, G. J. H.; Holscher, A. A. *Surf. Sci.* **1966**, *5*, 221–229.

(9) Andersson N Broms, P Yu, N Lupo, D Salaneck, WR, a J. *Adv. Mater.* **1998**, *10*, 859.